Papers submitted to the Conference "Applications of Physics in Mechanical and Material Engineering"

Influence of the Number of Meta-Atom Layers on the Occurrence of Local Resonances in Phononic Structures

S. Garus*

Department of Mechanics and Fundamentals of Machinery Design,
Faculty of Mechanical Engineering and Computer Science,
Czestochowa University of Technology, Dąbrowskiego 73, 42-201 Częstochowa, Poland

Doi: 10.12693/APhysPolA.142.124 *e-mail: sebastian.garus@pcz.pl

In order to investigate the effect of the number of meta-atomic layers on the propagation of the mechanical wave, studies on the propagation of the Gaussian impulse in structures with from one to five five-atomic layers in the phononic structure were carried out. The structure consisted of square-section meta-atoms made of polylactic acid. Wave propagation was analyzed using the finite difference time domain and fast Fourier transform algorithms. The conducted research showed the appearance of local resonance fields in the inter-meta-atomic space, resulting from the phenomena of diffraction and interference, which reduced the speed of wave propagation in the structure and caused the occurrence of gaps in the analyzed quasi-two-dimensional structures.

topics: acoustic barriers, FDTD, fast Fourier transform (FFT), local resonance

1. Introduction

In order to determine the band gap for phononic structures, the frequency response in the analyzed frequency range of mechanical waves should be determined. There are many methods that can be used for this purpose, for example, the one-dimensional transmission line model (TLM) [1], the eigenmodes matching theory (EMMT) [2], multiple scattering theory (MST) [3, 4], the plane wave expansion method (PWE) [5–7], the plane wave finite element (PWFE) [8], the finite element method (FEM) [9–11], the boundary element method (BEM) [12, 13], the boundary integral equation method (BIEM) [14], the unfitted Nitsche's method [15], the local radial basis function collocation method without mesh (LRBFCM) [16], the transmission matrix method (TMM) [17–20], and, among others, the finite difference time domain (FDTD) algorithm [21–23].

The study investigated the effect of the number of meta-atom layers in two-dimensional phononic structures on the propagation of the Gaussian impulse.

2. Finite difference time domain

Mechanical wave propagation is described by a system of differential equations, which consists of the continuity equation and the Euler equation, as, respectively,

$$\begin{cases} \frac{1}{\rho c^2}\frac{\partial p(\boldsymbol{x},t)}{\partial t} = -\nabla\cdot\boldsymbol{v}\left(\boldsymbol{x},t\right), \\ \rho\frac{\partial \boldsymbol{v}(\boldsymbol{x},t)}{\partial t} = -\nabla p\left(\boldsymbol{x},t\right), \end{cases} \tag{1}$$

where $p(\boldsymbol{x},t)$ is the pressure field in Cartesian space $\boldsymbol{x}$ and time t, $\boldsymbol{v}(\boldsymbol{x},t)$ is the vector velocity field, ρ and c are respectively the density and the phase velocity of the mechanical wave propagating in the material.

The gradient was defined as

$$\nabla\cdot\boldsymbol{F} = \left(\frac{\partial F}{\partial x_1}, \frac{\partial F}{\partial x_2}, \cdots, \frac{\partial F}{\partial x_n}\right), \tag{2}$$

and the divergence specified for a Cartesian space is

$$\nabla\cdot\boldsymbol{F} = \left(\frac{\partial}{\partial x}, \frac{\partial}{\partial y}, \frac{\partial}{\partial z}\right)\cdot(F_x, F_y, F_z) = \frac{\partial F_x}{\partial x} + \frac{\partial F_y}{\partial y} + \frac{\partial F_z}{\partial z}. \tag{3}$$

Using (2) and (3) and transforming the system of equations into a two-dimensional case, the following result was obtained

$$\frac{\partial p}{\partial t} = -\rho c^2\left(\frac{\partial v_x}{\partial x} + \frac{\partial v_y}{\partial y}\right), \tag{4}$$

$$\frac{\partial v_x}{\partial t} = -\frac{1}{\rho}\frac{\partial p}{\partial x}, \tag{5}$$

$$\frac{\partial v_y}{\partial t} = -\frac{1}{\rho}\frac{\partial p}{\partial y}, \tag{6}$$

After converting the derivatives into difference equations and the discretization of space into a two-dimensional form, the following result was obtained

$$p|_{i,j}^{t+1} = p|_{i,j}^{t} - \rho|_{i,j}\left(c|_{i,j}\right)^2 \frac{\Delta t}{\Delta z} \times \left(v_x|_{i,j}^{t+\frac{1}{2}} - v_x|_{i-1,j}^{t+\frac{1}{2}} + v_y|_{i,j}^{t+\frac{1}{2}} - v_y|_{i,j-1}^{t+\frac{1}{2}}\right), \quad (7)$$

$$v_x|_{i,j}^{t+\frac{1}{2}} = v_x|_{i,j}^{t-\frac{1}{2}} - \frac{1}{\rho|_{i,j}} \frac{\Delta t}{\Delta z}\left(p|_{i+1,j}^{t} - p|_{i,j}^{t}\right), \quad (8)$$

$$v_y|_{i,j}^{t+\frac{1}{2}} = v_y|_{i,j}^{t-\frac{1}{2}} - \frac{1}{\rho|_{i,j}} \frac{\Delta t}{\Delta z}\left(p|_{i,j+1}^{t} - p|_{i,j}^{t}\right), \quad (9)$$

The notation $p|_{i,j}^{t}$ determines the pressure value at a point in space defined by coordinates i and j at the moment of time t. To ensure stabilization of the simulation, the Courant condition must be satisfied, which connects (after discretization) step in time Δt with step in space Δz and the maximum phase velocity $c_{\max}$ in the simulation of the problem under consideration. The Courant condition for a two-dimensional problem is defined as

$$\Delta t < \frac{1}{c_{\max}\sqrt{\frac{1}{(\Delta x)^2} + \frac{1}{(\Delta y)^2}}}. \quad (10)$$

For a square mesh, where $\Delta z = \Delta x = \Delta y$, a stable simulation is obtained with the assumption

$$\Delta t = \frac{\Delta z}{2c_{\max}}. \quad (11)$$

The perfect matched layers (PML) algorithm was used to suppress the wave at the boundary of the simulation area and to prevent internal reflections of the waves. Time domain signals are transformed into the frequency domain using a discrete Fourier transform (DFT) which allows the band gap range, the signal power spectrum, and transmission to be determined.

3. Results and discussion

The parameters necessary to initiate the FDTD algorithm include the maximum speed $c_{\max}$ of mechanical wave propagation in the simulation, the minimum wavelength $\lambda_{\min}$, and the parameters related to the discretization of space and simulation time, Δz and Δt, respectively.

In this work, the ambient material was air with a density of $\rho_a = 1.29$ kg/m^3 and the speed of sound propagation $c_a = 331.45$ m/s, and the material from which meta-atoms were constructed was assumed to be polylactic acid (PLA) with a density of $\rho_m = 1240$ kg/m^3 and the speed of sound propagation $c_m = 2220$ m/s [24–26].

In order to maintain the stability of the simulation of the FDTD algorithm used, and at the same time to optimize the computation time, the highest wave propagation velocity was adopted during the calculations, equal to $c_{\max} = 2300$ m/s, which must be greater than the highest value of the wave phase velocity for the materials used in the simulation.

Taking into account air as the medium material, the minimum speed of wave propagation was defined as $c_{\min} = 330$ m/s. By using dependencies

$$\lambda_{\min} = \frac{c_{\min}}{f_{\max}}, \quad (12)$$

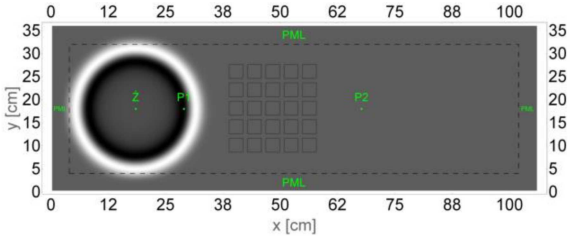

Fig. 1. Pressure distribution over 1000 time steps.

where $f_{\max} = 4$ kHz is the upper range of acoustic frequencies, the minimum propagating wavelength was determined as $\lambda_{\min} = 8.25$ cm. The recommended step of space discretization should be at least ten times smaller than the minimum wavelength [27]. In order to increase the accuracy of the calculations, the spatial step $\Delta z = 2.5$ mm was adopted (the upper range of acoustic frequencies for this step is 13.2 kHz), which, after substituting for the Courant stability condition (see (11)), gives the time step equal to $\Delta t = 5.43 \times 10^{-7}$ s. The source of the acoustic wave Z was located 18.5 cm from the left edge of the simulation, and points P1 and P2 were at a distance of 29 and 67.75 cm, respectively. Points Z, P1, and P2 were located 18 cm from the lower limit of the simulation area. The dimensions of the space of the simulation area were 36 cm on the vertical axis and 106 cm on the horizontal axis. There was a four-centimeter PML layer around the simulation area.

The Gaussian impulse IG used for the successive values of the time step T was described by the relationship

$$IG(T) = \sin\left(3000\pi\, T\Delta t\right) \exp\left[-0.2\left(\frac{305-T}{50}\right)^2\right]. \quad (13)$$

A soft source has been defined as

$$\mathrm{Z}|_{x,y}^{T} = \mathrm{Z}|_{x,y}^{T-1} + IG(T). \quad (14)$$

In the first stage of the work, the disturbance of the medium propagated in a structure with a regular system, consisting of 5 columns and 5 rows of square-shaped meta-atoms with a side of 3 cm and a lattice constant of 4 cm. The pressure distribution after 1000 simulation steps for a soft Gaussian spring is shown in Fig. 1.

Figure 1 shows the source point of the mechanical wave Z and the first and second measuring points, P1 and P2, respectively. The dashed line marks the area of the PML boundary conditions, in which the mechanical wave quenching took place. The figure shows the structure of meta-atoms. The highest pressure values at a given moment in time are marked in white, and the lowest in black.

Contrary to phononic crystals, where the infinite periodicity of meta-atoms (periodic boundary conditions) is analyzed, in real realizations of phonic structures, the number of elements is finite and defined in the studied area. Research on the

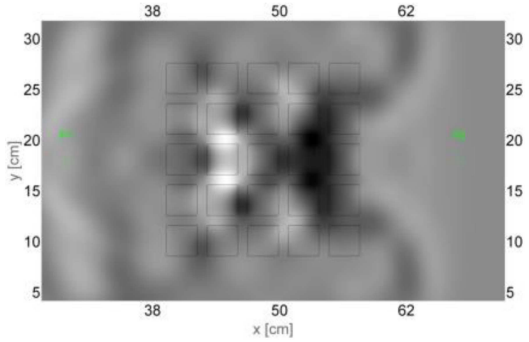

Fig. 2. Pressure distribution over 3000 time steps.

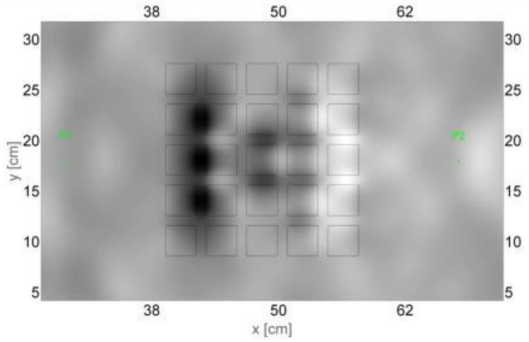

Fig. 3. Pressure distribution over 5000 time steps.

propagation of mechanical waves in phononic structures is carried out by analyzing the time series at selected points in space and by using discrete Fourier transforms, and on their basis obtaining the power spectrum as a function of frequency.

Figures 1, 2, and 3 show the pressure distribution in the analyzed space after 1000, 3000, and 5000 time steps, respectively. The wave impulse propagating in the structure causes the formation of local areas of increased pressure in the inter-meta-atomic spaces, which are caused by the phenomena of diffraction and interference of waves inside the structure. These local enhancements of the pressure distribution of the media lead to a slower propagation of the wave passing through the structure in relation to the surrounding wave, as can be seen in Fig. 2. Further iterations of the algorithm (Fig. 3) showed decreasing values of pressure amplitudes and the continuous occurrence of local areas of increased pressure, which contributed to the propagating disturbances of this field.

Figure 4 shows the time series of pressure values at measurement points P1 and P2 for 6000 steps of the algorithm. At point P1, there is a superposition of the generated and reflected pulses. Further fluctuations in the pressure value occured as a consequence of diffraction phenomena and interferences within the structure. The reduced amplitude value of the signal from the point P2 is related to the wave scattering in the two-dimensional space and, as a consequence, to the reflection of the pulse from the phononic structure.

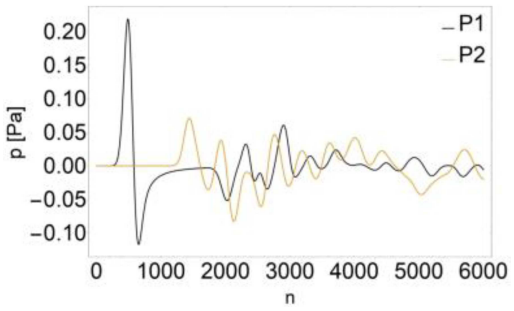

Fig. 4. Time series of pressure values at measuring points P1 and P2.

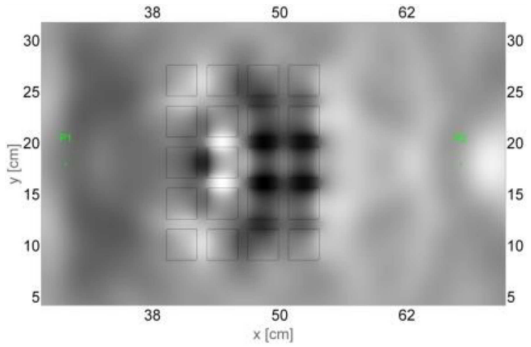

Fig. 5. Pressure distribution for the four layers of meta-atoms.

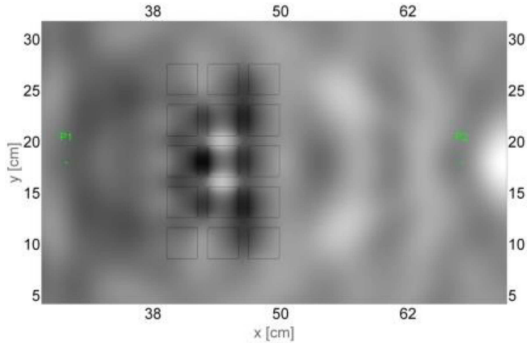

Fig. 6. Pressure distribution for the three layers of meta-atoms.

In order to investigate the influence of the number of meta-atom layers on the propagation of the mechanical wave, the Gaussian impulse propagation was carried out in structures with four (Fig. 5), three (Fig. 6), two (Fig. 7), and one (Fig. 8) five-atomic layers in the phononic structure. The structure consisted of meta-atoms, with a square cross-section of 3 cm, made of PLA, and with a lattice constant of 4 cm. The pressure distributions in Figs. 5–8 are shown after 5 000 time steps.

In all analyzed cases, part of the wave impulse energy was reflected from the surface of the first meta-atom layer.

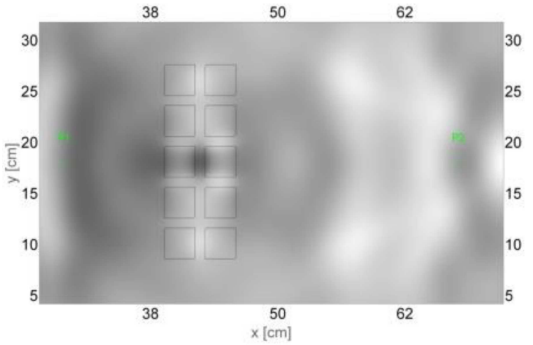

Fig. 7. Pressure distribution for two layers of meta-atoms.

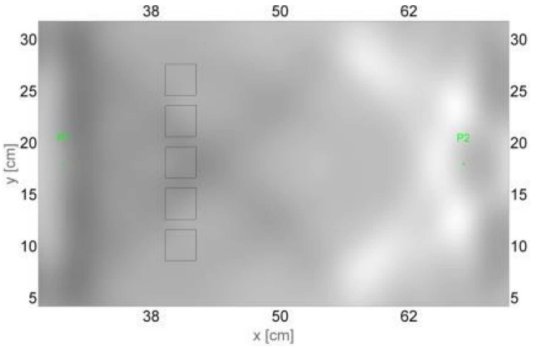

Fig. 8. Pressure distribution for one layer of meta-atoms.

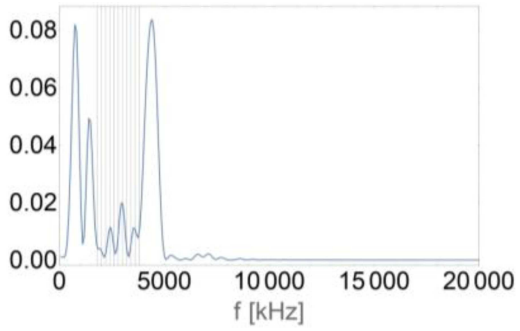

Fig. 9. Power spectrum for the five layers of meta-atoms.

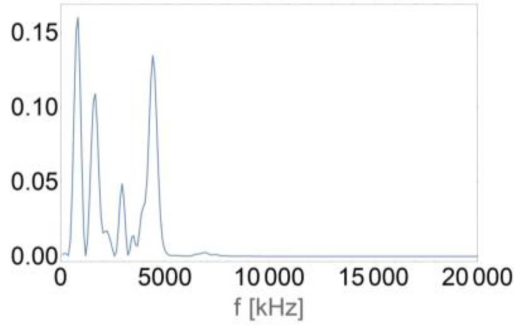

Fig. 10. Power spectrum for the four layers of meta-atoms.

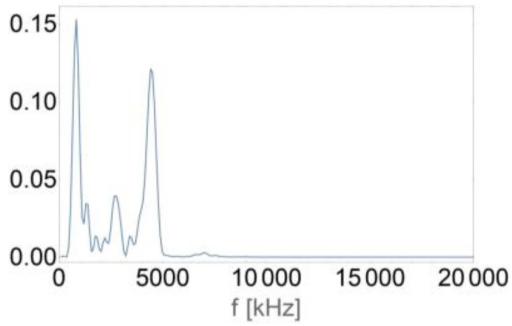

Fig. 11. Power spectrum for the three layers of meta-atoms.

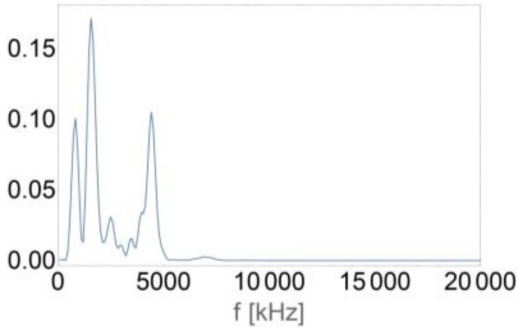

Fig. 12. Power spectrum for two layers of meta-atoms.

For structures with one and two meta-atom layers (Figs. 7, 8), part of the wave impulse energy propagated through the structure without creating local fields of increased pressure between the meta-atoms, and diffraction at the boundaries of the structure's layers caused a moving focus of the wave impulse on the line connecting the source and measurement points. On the other hand, from three layers in the structure (Figs. 3, 5–7), local fields of increased pressure in the interatomic spaces appeared, which reduce the speed of the wavefront by the structure and its energy for selected frequency ranges.

Figures 9–13 show the power spectra of signals at measurement points P2 after 5000 time steps for five (Fig. 9), four (Fig. 10), three (Fig. 11), two (Fig. 12), and one (Fig. 13) layer of the phononic structure. In the power spectra for the P2 point, one can notice the presence of reduced transmission bands in the frequency range from 1.8 to 3.8 kHz, which is not present for a single layer of meta-atoms. As the number of layers increased, the width of this band was observed to increase. The characteristic of the mechanical wave power spectrum at point P2 for the structure with four layers (Fig. 10) is similar to the characteristic shown in Fig. 9. Adding another layer resulted in an almost two-fold reduction in the value of the power spectrum peaks.

In the power spectra of the transmitted mechanical waves (P2), there were almost no frequency components above 5 kHz. As the conducted research

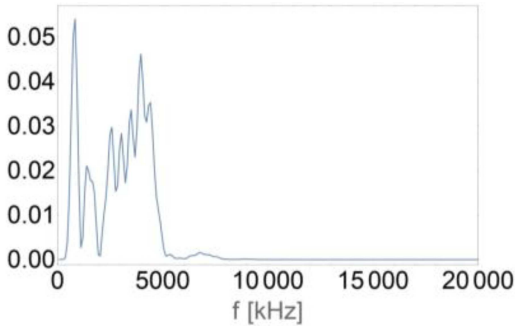

Fig. 13. Power spectrum for one layer of meta-atoms.

showed, the frequency band in which the intensity of mechanical waves was reduced was present for two layers of meta-atoms. The structure with five layers of meta-atoms presented in Fig. 9 was the most advantageous. A wide band gap was obtained, marked with vertical lines.

4. Conclusions

The analysis of mechanical wave propagation was carried out using the FDTD algorithm, and the power spectra were obtained from the results of the discrete Fourier transform of the time series of pressure changes at selected measurement points.

As part of the research, the presence of local areas of increased pressure amplitude (local resonances) of the propagating mechanical wave in the inter-meta-atomic spaces within the phononic structure was demonstrated, which reduced the amplitude of selected frequency ranges of the mechanical wave transmitted by the structure.

As shown by the research on the effect of the number of meta-atom layers in the structure, the reduced intensity of mechanical waves was already present for two meta-atom layers, with the structure with five meta-atom layers being the most advantageous.

References

[1] L. Luschi, F. Pieri, *Proc. Eng.* **47**, 1101 (2012).

[2] H. Zhang, B. Liu, X. Zhang, Q. Wu, X. Wang, *Phys. Lett. A* **383**, 2797 (2019).

[3] C. Qiu, Z. Liu, J. Mei, M. Ke, *Solid State Commun.* **134**, 765 (2005).

[4] J. Mei, Z. Liu, J. Shi, D. Tian, *Phys. Rev. B* **67**, 245107, (2003).

[5] M. Sigalas, E. N. Economou, *Solid State Commun.* **86**, 141 (1993).

[6] M. S. Kushwaha, P. Halevi, G. Martínez, L. Dobrzynski, B. Djafari-Rouhani, *Phys. Rev. B* **49**, 2313 (1994).

[7] J. A. Kulpe, K. G. Sabra, M.J. Leamy, *J. Acoust. Soc. Am.* **137**, 3299 (2015).

[8] J.-F. Lu, J. Cheng, Q.-S. Feng, *Eur. J. Mech. A Solids* **91**, 104426 (2022).

[9] A. Khelif, B. Aoubiza, S. Mohammadi, A. Adibi, V. Laude, *Phys. Rev. E* **74**, 046610 (2006).

[10] X. Pu, Z. Shi, *Soil Dyn. Earthq. Eng.* **121**, 75 (2019).

[11] C. Zhao, J. Zheng, T. Sang, L. Wang, Q. Yi, P. Wang, *Constr. Build. Mater.* **283**, 122802 (2021).

[12] F.-L. Li, C. Zhang, Y.-S. Wang, *Eng. Anal. Bound. Elem.* **131**, 240 (2021).

[13] Q. Wei, X. Ma, J. Xiang, *Eng. Anal. Bound. Elem.* **134**, 1 (2022).

[14] M.V. Golub, O.V. Doroshenko, S.I. Fomenko, Y. Wang, C. Zhang, *Int. J. Solids Struct.* **212**, 1 (2021).

[15] H. Guo, X. Yang, Y. Zhu, *Comput. Methods Appl. Mech. Eng.* **380**, 113743 (2021).

[16] H. Zheng, C. Zhou, D.-J. Yan, Y.-S. Wang, C. Zhang, *J. Comput. Phys.* **408**, 109268 (2020).

[17] S.-H. Jo, H. Yoon, Y.C. Shin, B.D. Youn, *Int. J. Mech. Sci.* **193**, 106160 (2021).

[18] S. Garus, W. Sochacki, *Wave Motion* **98**, 102645, (2020).

[19] Yang Jin, Xin-Yu Jia, Qian-Qian Wu, Xiao He, Guo-Cai Yu, Lin-Zhi Wu, Bailu Luo, *J. Sound Vib.* **521**, 116721 (2022).

[20] A. Mehaney, A.M. Ahmed, F. Segovia-Chaves, H.A. Elsayed, *Optik* **244**, 167546 (2021).

[21] M.M. Sigalas, N. García, *J. Appl. Phys.* **87**, 3122 (2000).

[22] J.-H. Sun, T.-T. Wu, *Phys. Rev. B* **76**, 104304 (2007).

[23] N. Aravantinos-Zafiris, F. Lucklum, M.M. Sigalas, *Ultrasonics* **110**, 106265 (2021).

[24] D. Tarrazó-Serrano, S. Castiñeira-Ibáñez, E. Sánchez-Aparisi, A. Uris, C. Rubio, *Appl. Sci.* **8**, 2634 (2018).

[25] S. Yang, W.-D. Yu, N. Pan, *Phys. B: Condens. Matter* **406**, 963 (2011).

[26] Y. Wang, W. Song, E. Sun, R. Zhang, W. Cao, *Phys. E: Low-Dimen. Syst. Nanostruct.* **60**, 37 (2014).

[27] D.M. Sullivan, *Electromagnetic Simulation Using the FDTD Method: Sullivan/Electromagnetic Simulation Using the FDTD Method*, John Wiley & Sons, Hoboken (NJ) 2013.